Biogeosciences, 23, 4113–4132, 2026
https://doi.org/10.5194/bg-23-4113-2026

Biogeosciences Open Access EGU

How does biotic weathering work? Influence of alpine plants on rock temperature and rock moisture

Oliver Sass[1], **Urte Bauer**[1], **Anke Jentsch**[2], **and Thomas Deola**[2]

[1]Chair of Geomorphology, University of Bayreuth, 95447 Bayreuth, Germany
[2]Chair of Disturbance Ecology, University of Bayreuth, 95447 Bayreuth, Germany

Correspondence: Oliver Sass (oliver.sass@uni-bayreuth.de)

Received: 13 December 2025 – Discussion started: 27 January 2026
Revised: 15 April 2026 – Accepted: 15 April 2026 – Published: 22 June 2026

Abstract. Rock temperature and moisture are critical factors influencing rock weathering. In alpine environments, these parameters are determined by both macroscale factors, including climate, and microscale factors, including vegetation cover. We investigate the effects of alpine plant species with distinct architectures – among others *Dryas octopetala L., Primula auricula L.* and *Carex firma Scop.* – on rock temperature and moisture at rocky limestone slopes. The Arnspitze massif (German/Austrian border) was affected by severe wildfires in the 1940ies so that wide slope areas in the subalpine belt are still characterised by limestone outcrops free from forest cover.

Rock temperature and electrical resistivity (as a proxy for moisture) were monitored over three months at hourly resolution, complemented by small-scale electrical resistivity tomography (ERT) and microwave sensing (MW). Bare rock, soil-covered rock (<10 cm), and plant-covered rock with different species were compared.

Plant cover was found to reduce the mean daily temperature amplitudes in the rock by 3.2 to 5.2 K and change rates by up to 7 K h^{-1} compared to uncovered rock. Soil cover effects vary, influenced by soil thickness and microtopographic exposure. Varying rock temperature dynamics are attributed to plant architecture, with shading, canopy heating, decoupling from atmospheric conditions and rock moisture content hypothesized as key factors. Rock moisture increases under soil and plant cover, with reduced evaporation and altered drainage patterns assumed as driving mechanisms. ERT measurements reveal high spatial heterogeneity in rock moisture at the microscale, which is influenced by plant cover, and which is providing favourable sites for vegetation establishment. MW measurements show heightened moisture content under plants at shallow depth (few cm), while with further increasing depth, rock moisture decreases in plant covered rock, suggesting possible plant water uptake with different responses depending on species and functional types.

Regarding biotic rock weathering we hypothesize that plant cover generally mediates direct temperature cracking by reducing temperature extremes, but enhances chemo-physical subcritical cracking through increased moisture levels. This underscores how sparse alpine vegetation potentially influences microscale weathering processes.

1 Introduction

Weathering is a critical process in nature, as it serves as the starting point for erosion processes and soil formation. The intensity of weathering is further determined by factors such as time, climate, topography, and vegetation (Derry, 2009). Freeze-thaw weathering and temperature weathering are typical processes of physical weathering occurring on steep rock slopes in alpine environments. In freeze-thaw weathering, the volumetric expansion of ice and ice segregation increase tensional stress at crack tips in the rock, leading to rock fracture (Hales and Roering, 2007; Deprez et al., 2020; Draebing and Mayer, 2021). In temperature weathering, warming and cooling of rock is induced by wind and solar radiation, resulting in thermal stress fatigue over time (Hall, 1999). Almost all weathering processes are accelerated by abundant rock moisture, be they physical (frost cracking, Mitchell and Sass, 2024; salt weathering, Godts et al., 2023), chemical (hydration, oxidation; Calabrese and Porporato, 2020) or biological (biofilm; Gaylarde, 2020). Moisture plays a "dual role"

as it not only intensifies the abovementioned processes but is also of central importance for subcritical cracking (Eppes and Keanini, 2017), which is accelerated by rock moisture due to chemophysical bond breaking (Eppes et al., 2020). However, information regarding the internal moisture levels of bedrock under soil are limited (McAllister et al., 2017).

Rock weathering shapes ecosystem properties, thereby driving plant colonization and vegetation dynamics. In turn, it has been accelerated by plants for the last 400 million years (Porder, 2019). The contribution of plants to weathering is indirect by mediating energy and water fluxes, and direct by destructive root action (Table 1). Dense vegetation and soil cover generally protect surfaces by mitigating the erosive forces of wind and water (Dahanayake et al., 2024), while sparse vegetation provides less protection, increasing vulnerability to these forces (Starke et al., 2020). Furthermore, plant cover buffers temperature maxima and fluctuations in the rock subsurface (He et al., 2024). In the context of climate resilience of cities, the body of literature on vertical greening and its micro-climatic effects is steadily growing (see review in De Groeve et al., 2024). For example, ivy foliage was found to buffer thermal cycles, which considerably reduces the number and severity of freezing events (Coombes et al., 2018). However, studies from alpine rockwalls and related to biotic weathering are rare. The shadow of a single plant and the release of litter decrease the solar insolation at the surface, reduce the thermal radiation of the underground, and inhibit the influence of wind. Since specialized alpine plants accumulate heat in the canopy and topsoil, the temperature on rocks under low growing vegetation is decoupled from the atmosphere (Körner, 2021).

The influence of plant cover on subsurface moisture and the associated feedback loops are much less straightforward. Ni et al. (2019) found strong seasonal variations: water contents in vegetated semi-arid soils in summer were up to 50 % lower than in a bare soil due to higher evapotranspiration, while in autumn, water content in vegetated soil was up to 70 % higher. In an arctic-alpine setting, volumetric water content was found to vary by more than 50 % over meter-distances due to the spatial heterogeneity of soil-plant systems (Aalto et al., 2013). On calcareous slopes, different plant functional types exploit distinct water pools: a shallow-rooted shrub rely on variable, surface-level sources, whereas a deeper-rooted tree can also access more stable, deeper pools (Nie et al., 2019). Small-scale studies on moisture distribution in rock are very rare (e.g. Sass, 2004).

On sparsely vegetated rock slopes, cracks facilitate physical and chemical weathering processes. Plants can access continuous water supply and avoid drought when they are able to explore the cracks with their root system (Zwieniecki and Newton, 1995; Rempe and Dietrich, 2018; McCormick et al., 2021). Feedback loops occur as the scattered colonization of rocks by vascular plants favours the accumulation of soil and organic matter which can capture additional water (Kuntz and Larson, 2006). Many vascular plant species in alpine environments are adapted to a temporary drought phase with storage tissues in different plant parts like roots and leaves, yet constant water availability may be a precondition for their establishment (Körner, 2021). In cracks colonized by plants, the temporal and spatial patterns of water infiltration are altered compared to bare cracks, and infiltration rate increases. Once roots have entered the rock through a crack, biochemical weathering may be enhanced by moisture fluxes along the root (Pawlik et al., 2016). On the other hand, interception by the vegetation layer can temporarily retain water before it reaches the surface, with part of it being lost through evaporation (Klamerus-Iwan et al., 2020).

It is generally agreed that woody roots may split rock masses by physically prying them apart (Porder, 2019). Although the tensile strength of unweathered rock greatly exceeds the pressure achieved by radial root growth, fissures or chemically altered joints provide entrance routes (Pawlik et al., 2016) or concentrate roots within fractures (Witty et al., 2003). Additionally, roots release organic acids and mucilage at the fine root tips (Körner, 2021), which promotes chemical weathering (Liu et al., 2021; Larsen et al., 2023). In their literature review, Pawlik et al. (2016) state that knowledge on the process of root cracking is fragmentary. Present-day weathering caused by root action has been documented on two tree species. *Taxus baccata* L. expands its root system on fissures favouring cliff recession, then, once exposed to open air, stabilizes the vertical cliff face (Jackson and Sheldon, 1949). *Quercus muhlenbergii* Engelm. penetrates into the rock, accelerating dissolution and inducing rock displacement – processes not observed in similar adjacent rock outcrops with grass vegetation (Phillips, 2016). Studies on biomechanical weathering by vascular plants on alpine environments, that are not trees by growth form definition, are altogether missing.

Rock weathering, be it purely physical or supported by biochemical processes, provides niches for growth in rocky alpine environments, with the pioneer plants mediating weathering by modifying micro-climate. This co-evolution is a paradigm of biogeomorphological interaction (Viles et al., 2008; Marston, 2010; Eichel et al., 2016), on the fringe between the dominance of physical forcing to biogeomorphologic macroevolution (Corenblit et al., 2011, Fig. 8). In the deep time perspective, there is a large number of studies on the global consequences of enhanced weathering by the roots of emerging tree species in the Late Devonian (Algeo et al., 1995). However, there is a lack of local studies with a focus on the direct plant-rock relationship. It is unknown how strongly the cover of sparse, individual plants affects rock temperature and moisture, key parameters when evaluating the weathering dynamics of an area (Hall, 1999). We expect that plants will alter the residence time and the amount of moisture inside the rock, altering infiltration and evaporation. The latter can increase or decrease because plant cover can change solar radiation, air pressure, air humidity, and wind influence at the rock surface.

Table 1. Hypothetical influence of vegetation on weathering processes (enhancing +, attenuating −).

Process of rock decay	Potential influence of plants	Effect
Frost cracking	Constant water availability; attenuation of temperature amplitude	+; −
Thermal cracking	Attenuation of temperature amplitude	−
Salt crystallization/hydration	Delaying or preventing salt crystallization by inhibiting desiccation	−
Chemical weathering	Constant water availability, release of organic acids, lower outflow of weathering products	+, +, −
Solution (karstification)	Constant water availability; water loss by transpiration and interception; release of organic acids	+; −; +
Root cracking	Root thickness growth, widening of cracks	+
Subcritical cracking	Water availability; root length growth; release of organic acids	+

To fill this research gap, we investigated variations in rock temperature and rock moisture beneath seven different vascular plant species belonging to different functional types (life form, growth form, and root architecture). While life forms impose general constraints on plant stature, determining the position of perennating buds, the variety of growth forms captures finer-scale differences in above-ground architecture and ramification patterns, while root architecture affects water uptake (e.g. Körner, 2021). This combination is thereby expected to capture a range of plant–substrate interaction strategies relevant for rocky outcrop vegetation, extending beyond the specific biogeographic context of the subalpine rocky slopes in the European Alps investigated in this study. Specifically, our research questions include:

i. Is the daily temperature amplitude in the rock reduced by vegetation and soil cover, potentially reducing thermal stresses?

ii. Does rock moisture increase with vegetation and soil cover, potentially enhancing chemical weathering, karstification and subcritical cracking?

iii. Are changes in rock moisture dominated by rain events, with vegetation and soil cover defining the water residence time and reaction strength, and the drying process afterwards?

iv. Is the influence of plants on moisture patterns in the rock – in intensity, depth and extent – highest for dense, ground covering plant forms, such as mat-forming dwarf-shrubs, and decreases in sparsely covering plant forms, such as herbaceous rosettes and thin, erect dwarf shrubs?

2 Study site

This study was carried out at the Arnspitze, an isolated mountain range northwest of Innsbruck, between the Karwendel and the Wetterstein mountains. These mountain ranges are part of the Northern Calcareous Alps, which extend across Germany (Bavaria) and Austria (Tirol). The highest peak of the Arnspitze range is the Great Arnspitze, with an elevation of 2196 m above sea level (a.s.l.) (Sass and Kloss, 2015). The study sites were located on the southern (Tirol) and eastern slope (Bavaria) of the Arnspitze (Fig. 1).

The Arnspitze lies between the suboceanic, cool, and humid northern side of the European Alps and the subcontinental, warm, and dry Inn Valley. The mean yearly precipitation in the nearby valley of Scharnitz (976 m a.s.l.) is 1734 mm and the mean temperature is 3.3 °C. Most precipitation falls in summer as rain (May–August > 200 mm per month); the driest month is February with 88 mm. The mean monthly temperature varies during the year from −7 °C in January to 12.6 °C in July (a range of 19.6 °C). In Winter and spring, dry foehn winds are typical of the region (Vacik et al., 2011).

The geology of the area is dominated by the light-grey Wetterstein limestone dating to the Middle Triassic, which is mostly massive or thick-bedded. With a calcium carbonate content of 95 %–99 % the Wetterstein limestone is very pure and is prone to intense karstification. As a result, there are no perennial watercourses and overland flow is limited even during heavy rainfall (Sass et al., 2010), so direct rainfalls are the main source of rock moisture (Sass, 2005).

Due to the low amount of solution residue, raw humus carbonate soils and shallow rendzinas with typical Ah-C or O-C profiles are formed (Sass et al., 2019). On the southern and eastern slopes of the mountain, wildfires burnt the forest and the organic layers, leaving these areas highly exposed. The erosion and deposition rates of debris caused by avalanches

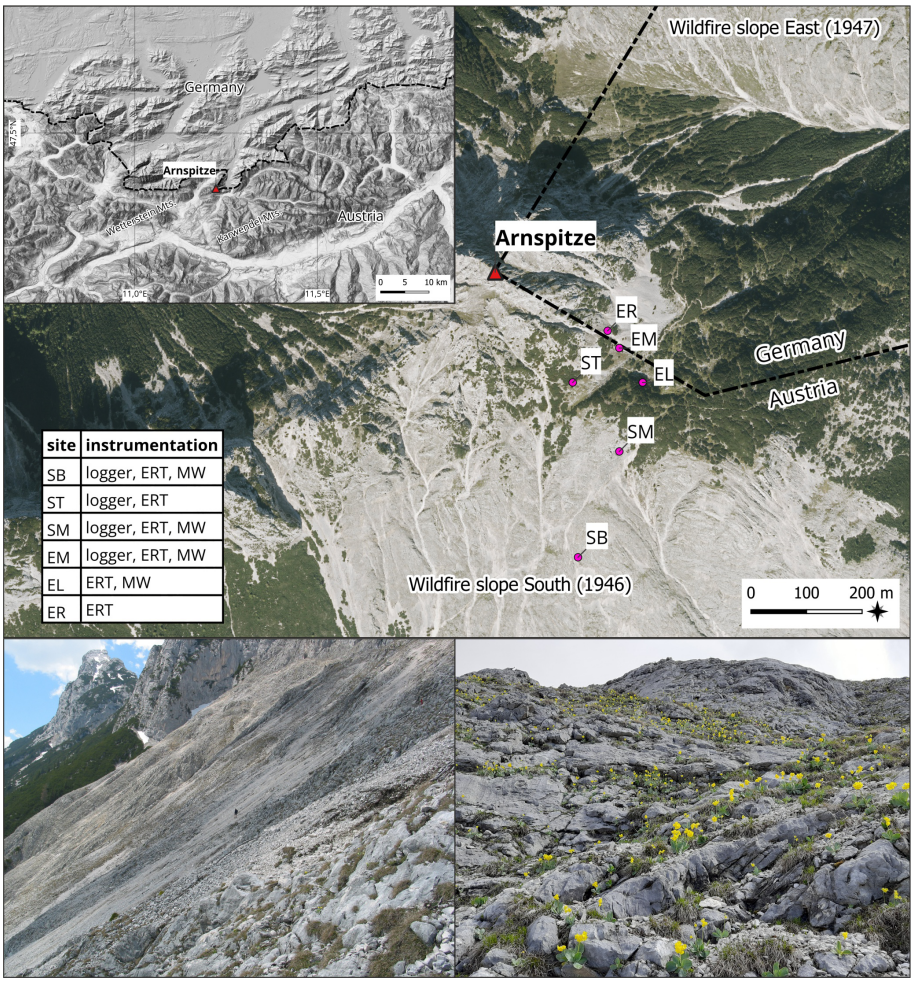

Figure 1. Location of the study area at the border between Germany and Austria (top left) and the study sites on the slopes of the Arnspitze; Background: OpenStreetMap (top left); hillshade and contourlines processed from digital terrain model of the state of Tyrol (https://data.tirol.gv.at, last access: 2 December 2024). Photos from the south-facing slope by OS.

remain consistently high (Sass et al., 2010), primarily disturbing tall flora and preventing the formation of thick soil layers (Sass and Sarcletti, 2017). A subalpine and alpine low-statured flora characterized by the shrub *Rhododendron hirsutum L.* and the creepy woody plants *Dryas octopetala L.* has established on the steeper parts of the slopes, growing mostly in rock cracks and places with minimal soil accumulation (De Giuli et al., 2024). The plant species associated with the microclimatic measurements are listed in Table 2.

3 Methodology

In total, six study sites were established on the eastern and southern slopes near the Arnspitze Hut. The sites ranged in elevation from 1790 to 2005 m a.s.l., with orientations varying between 92° E and 185° S (see Table 3). For each method applied (see Table 3), the aim was to obtain measurements from plant-covered and uncovered rock under as identical conditions as possible (e.g. exposure, inclination). At each of the four T/RM logger sites (see below), three measurement points were chosen close to each other. The first (reference) measurement point was always located in rock without plant cover; the second measurement point was in rock directly under the leaves or roots of one of the target species, or sometimes two species occurring in one place; the third measurement point was in rock with a varying cover situation depending on the location (see Table 3).

3.1 T/RM dataloggers

Four dataloggers manufactured at the University of Bayreuth, each equipped with three sensor pairs for measuring rock moisture (RM) by means of electrical resistivity and three integrated temperature sensors (T) were installed to capture detailed temporal patterns of rock temperature and moisture. The dataloggers measured electrical resistivity (ER) and T in the rock every minute, saving the average of the measure-

Table 2. Plant species at the study sites (H caesp = tufted hemicryptophyte, Ch rept = mat-forming chamaephyte, Ch suff = subshrubby chamaephyte, H ros = rosette hemicryptophyte, Ph caesp = tufted phanerophyte).

Species	Plant form	Aboveground architecture*	Root architecture*
Carex firma HOST	H caesp	forming dense cushions/tussocks, upright from the base, periodic reduction of shoots	base below surface, one main root and from there fine roots spreading
Dryas octopetala L.	Ch rept	woody dwarf shrub, shoot axis prostrate, often in large mats	Base below surface, branched root system of stronger and finer roots, clonal growth organs on oldiest part
Erica carnea L.	Ch suff	dwarf shrub, prostrate, branched, only woody at the base	base below surface, branched root system of stronger and finer roots
Globularia cordifolia L.	Ch rept	woody dwarf shrub, forms cushions of one individuum, creeping	base at the surface, branched well connected root system of stronger roots and finer roots spreading from them;
Helianthemum alpestre (JACQ.) DC.	Ch suff	dwarf shrub, forms cushions, only woody at the base	Base at surface, less connected root system of main and finer roots, clonal growth organs on oldiest part
Primula auricula L. *subsp. auricula*	H ros	base rosette with periodic reduction of shoots	one large tap root with finer roots spreading from there
Rhododendron hirsutum L.	Ph caesp	evergreen shrub, branched from the base	base below surface, branched root system of stronger and finer roots

* based on Kutschera and Lichtenegger (1982, 1992); Kutschera et al. (1997); Hassler and Muer (2022); InfoFlora (2024); Klimešová and Klimeš (2024).

Table 3. Instrumentation and location parameters of the study sites.

Study site	Elevation	Orientation	Instrumentation	Plants
South Bottom (SB)	1790 m	97° E	*T*/RM logger, rain, ERT, MW	*T*/RM: *Erica carnea, Carex firma* ERT: *C. firma, Primula auricula* MW: *E. carnea (2)*
South Middle (SM)	1940 m	147° SE	*T*/RM logger, ERT, MW	*T*/RM: *C. firma, moss (unspecified)* ERT: *C. firma, P. auricula*, moss (unsp.) MW: *G.cordifolia (SM ERT: 3), P. auricula (SM ERT: 3), C. firma (SM logger: 6)*
South Top (ST)	2005 m	185° S	*T*/RM logger, ERT	*T*/RM: *Dryas octopetala* ERT: *D. octopetala, C. firma*, *Helianthemum alpestre*
East Left (EL)	1960 m	46° NE	ERT, MW	ERT: moss (unsp.) MW: *Rhododendron hirsutum (EL: 4, EL2: 2)*
East Middle (EM)	1965 m	92° E	*T*/RM logger, ERT, MW	*T*/RM: *D. octopetala, C. firma* ERT: *D. octopetala* MW: *D. octopetala (6)*
East Right (ER)	1985 m	98° E	ERT	ERT: *D. octopetala, C. firma, R. hirsutum*

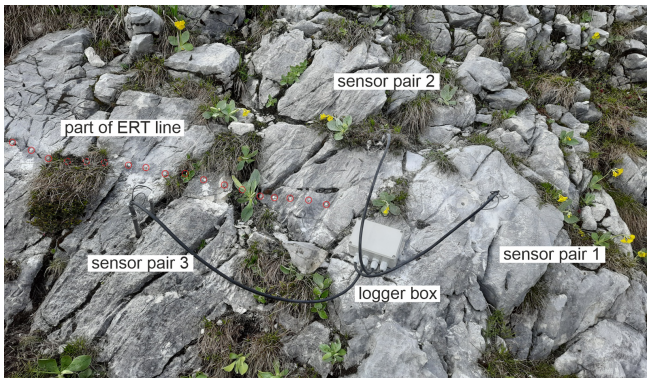

Figure 2. Field setup at the Bottom South site showing conductivity sensor pairs and part of the ERT electrode line (highlighted red).

ments every 10 min. At site SB, precipitation was also measured at a tipping gauge (one tip = 0.1 mm) connected to the datalogger, with the values summed continuously and the result saved every 10 min. As all sites were within a radius of approx. 500 m, one gauge was deemed sufficient to capture temporal precipitation patterns.

The ER of rock is a frequently used proxy for rock moisture (Sass, 2005; Mitchell and Sass, 2024). ER changes by orders of magnitude with water content, where a high rock water content corresponds to a low ER and vice versa. For the measurement, an electric current is introduced into the rock. Based on the applied current and generated voltage the resistivity is given in Ohm (Ω). In our study, positive and negative poles were switched once during the measurement to counteract polarization effects. Each measurement took about one second.

The measured ER is not only a function of water content but also of the measurement array, which means that the measurement in each specific array needs to be calibrated in laboratory tests. For measuring ER at the field sites, an electrode pair was installed in two boreholes (10 mm diameter, 50 mm deep) spaced 50 mm apart. To ensure tight and reliable electrical contact to the rock, metal, cylindrical expansion bolts (30 mm long) were inserted into the drillholes and fixed by hammer blows (Weiss and Sass, 2022). The sensor rods were screwed into the fixed bolts. Temperature sensors were integrated at the tip of one of the sensor rods of each pair, at a depth of approximately 30 mm under the rock surface (MAXIM DS 18B20 with an accuracy of ±0.5 K). Figure 2 shows the field setup at the South Bottom site.

Data quality is influenced by soluble ions in the pore water, temperature and the porosity of the rock. In a humid alpine setting far from sources of air pollution, soluble ions apart from $CaCO_3$ from the limestone are negligible. For the temperature influence, a correction factor of $0.022\,K^{-1}$ was applied which takes the increase of conductivity in the pore water into account (Weast et al., 1989). Varying porosity may lead to misinterpretation, as areas of high porosity can hold a higher absolute amount of water and thus appear to be wetter. Comparison between two sensor pairs should thus be treated with caution. Because of unknown porosity around the sensors, we refrained from applying a laboratory-derived resistivity-moisture conversion. ER measurements were transformed into conductivity (C) values using $C = ER^{-1}$ and corrected to a standardized temperature of 25 °C (Hayashi, 2004).

3.2 2D-Resistivity (ERT)

2D-resistivity is based on the same principle as single resistivity measurements, with the difference that 4-point measurements at numerous electrodes are combined to form a 2D resistivity profile of the subsurface. The principle is described in more detail by Dahlin (1996) or Schrott and Sass (2008). Applications on rock or stonework were presented e.g. by Leucci et al. (2007), Sass and Viles (2010), Suryanto et al. (2017) and Sass and Viles (2022). In our small-scale approach we used 25 electrodes at a spacing of 5 cm (total profile length: 1.2 m). The electrodes were 4 mm screws inserted into small metal plugs in 6 mm wide and 10 mm deep drill holes; this array provides stable and reliable electrical contact. In profiles with deeper soil layers, plugs and screws were embedded in the soil. The electrodes were connected to a Geotom ERT device using a specially manufactured cable with crocodile clips. The measurements were carried out by means of Wenner array (Loke, 1999) enabling a maximum penetration depth of approx. 25 cm. Data inversion was done using the Res2D/3DInv software.

Measurements were conducted in June 2024. Each ERT profile was arranged in a straight line, ideally at a 90° angle to the main fracture direction, with areas of bare rock and different plant cover situations (see Fig. 2 as an example). For better inversion results and interpretation, the microtopography of the profiles was recorded using a string and a folding ruler and implemented in the inversion routine.

3.3 Microwave (MW) sensors

Non-destructive moisture surveying using handheld MW sensors is common in built heritage surveys and is effective for quick surveys of spatial moisture distribution (Orr et al., 2020; Sass and Heil, 2024). In our study, the MOIST 350B by *hf sensor* was used. This sensor produces an electromagnetic wave and measures the proportion of energy that is reflected. The frequency range is around 2–3 GHz, in which the influence of salinity is negligible (Orr et al., 2020). Two sensor heads were employed: MOIST R1M, which penetrates up to 2–3 cm, and MOIST PM, which penetrates up to 25–30 cm according to the manufacturer. The sensor does not measure at a certain defined depth but integrates the volume from the surface down to the specified penetration depth (Weiss and Sass, 2022).

The sensor provides a dimensionless value (moisture index, MI) in a range from 0 to 4000. The data can be transformed into absolute values of volumetric water content in a lab procedure using large samples from the study area (Orr et al., 2020; Sass and Heil, 2024). However, as the reflectance to moisture conversion is linear (Piuzzi et al., 2018; Orr et al., 2020; Sass, 2022; D'Alvia et al., 2022), correct statements on relatively dry or wet are possible using the unconverted dimensionless MI values. The value ranges between the R1M and the PM sensor are completely different, thus, the values cannot be compared between the sensor heads.

Measurement points were chosen in the field under or around target plant species and in similar places without vegetation. The selected species (Table 4) are common in this environment (De Giuli et al., 2024). They span a diverse range of Raunkiaer's (1934) life forms, growth forms (e.g. reptant, caespitose, rosulate), and root architectures. To test whether root depth in our species pool is linked to Raunkiaer's growth forms, we queried the TRY database for rooting depth values (Kattge et al., 2020; accessed on 29 September 2025). Five repeated measurements were made at each measurement point to reduce errors due to irregular surfaces. For measurements below plant leaves and soil, the cover had to be (temporarily) removed. The measurements were taken below the plant leaves for all species except *Primula auricula L.*, where the plant leaves did not cover much space of the rock. There, measurements took place directly below the plant individual.

4 Results

4.1 Precipitation

From the start of measurements on 27 May to the end on 27 August, a total of 468.5 mm of rainfall was recorded. This period represents the peak local growing season. The majority of the rainfall occurred in June (254.6 mm), followed by July (159.6 mm), August (31.3 mm), and the few days recorded in May (23 mm). The amounts of rainfall were very similar to the weather station in the valley (Mittenwald: June: 239.2 mm, July: 177.7 mm, Aug: 71.9 mm; https://gkd.bayern.de, last access: 10 April 2025). The maximum daily rainfall was observed on 2 June, with 42.2 mm, while there was a total of 34 d without any recorded rainfall. Notably, August experienced the least rainfall, with 22 d without precipitation. In Mittenwald, the year 2024 (1384 mm) was slightly wetter than the mean of the preceding 10 years (2014–2023: 1291 mm).

4.2 Rock temperature

During the measurement period, the rock temperatures at approximately 3–5 cm depth fluctuate greatly, both for the absolute maxima and minima, as well as for the mean daily amplitude (see Fig. 3). The highest mean daily temperature amplitude, the absolute minima, and the absolute maxima in the measurement period occur for uncovered rock (Fig. 3) while plant-covered rock has the lowest amplitudes. An exception is uncovered rock at ST, where a soil-filled crack has the smallest mean daily temperature amplitude and the absolute minimum. Considering the maximum temperature gradient in the 10 min interval ($\Delta T/10\,\text{min}$) no clear trend can be seen for the different types of vegetation cover.

At all locations, the highest mean daily temperature amplitudes were consistently measured at uncovered rock. Besides this, the results differ slightly for each location (see Fig. 3). At SB there is no significant difference in mean daily temperature between uncovered rock and soil covered rock ($13.8 \pm 6.0\,°\text{C}$ vs $13.4 \pm 5.4\,°\text{C}$). With plant cover by the genera *Erica carnea* and *Carex firma*, the mean daily temperature ($10.5 \pm 4.3\,°\text{C}$) is significantly lower. At SM, the mean for uncovered rock ($12.1 \pm 5.1\,°\text{C}$) is significantly higher than for shaded rock with moss cover and rock covered by *Carex firma* while there is no significant difference between shaded rock and vegetation. At ST, uncovered rock shows the highest amplitude ($11.9 \pm 4.8\,°\text{C}$) followed by rock covered by *Dryas octopetala* and soil ($8.7 \pm 3.5\,°\text{C}$), and soil-filled cracks in last place ($6.7 \pm 3.0\,°\text{C}$). At EM, uncovered rock shows the highest amplitude ($10.9 \pm 5.1\,°\text{C}$). Of the two plant-covered points, the amplitudes in rock covered by *Dryas octopetala* leaves ($7.2 \pm 3.1\,°\text{C}$) are significantly greater than under a *Dryas-Carex* complex ($5.7 \pm 2.5\,°\text{C}$).

Thermal weathering is driven not only by the magnitude of diurnal temperature amplitude, but also by the rate of temperature change. Our data shows that the mean maximum heating rate is around $10\,\text{K}\,\text{h}^{-1}$ for the rock sites and only 2–$3\,\text{K}\,\text{h}^{-1}$ for the plant covered sites. The same is valid for the maximum cooling rate which is between -5 and $-10\,\text{K}\,\text{h}^{-1}$ for the rock sites and mostly between -1 and $-3\,\text{K}\,\text{h}^{-1}$ for vegetation sites. Two figures showing this are provided in the appendix (Figs. A1 and A2).

4.3 Rock moisture: progression of electrical conductivity

Measuring points on rock without vegetation tends to show the lowest mean electrical conductivity values (Fig. 4), which means that they are the driest. SB is an exception to this, here the rock under thin *Erica carnea – Carex firma* leaves is even drier. The thick carpet of leaves seems to keep off rainfall in this position without greatly inhibiting evaporation. At the three other sites, the mean conductivity of rock with vegetation cover is higher than that of uncovered rock. At SM, the mean conductivity of shaded/mossy rock is similar to the uncovered rock while it is markedly wetter under *Carex firma*. At ST, mean conductivity of the rock strongly increases from uncovered rock to rock covered by *Dryas octopetala*. At EM, the same pattern can be seen between uncovered rock and *Dryas octopetala*, albeit to a lesser degree; the *Dryas-Carex* complex is slightly wetter. Soil-filled cracks

Table 4. Measured plant species with the microwave sensor.

Plant species		plant form	locations	n
Dryas octopetala		Ch rept	EM	6
Globularia cordifolia		Ch rept	SM-ERT	3
Erica carnea		Ch suff	SB	2
Primula auricula		H ros	SM-ERT	3
Carex firma		H caesp	SM-logger	6
Rhododendron hirsutum		Ph caesp	EL	6

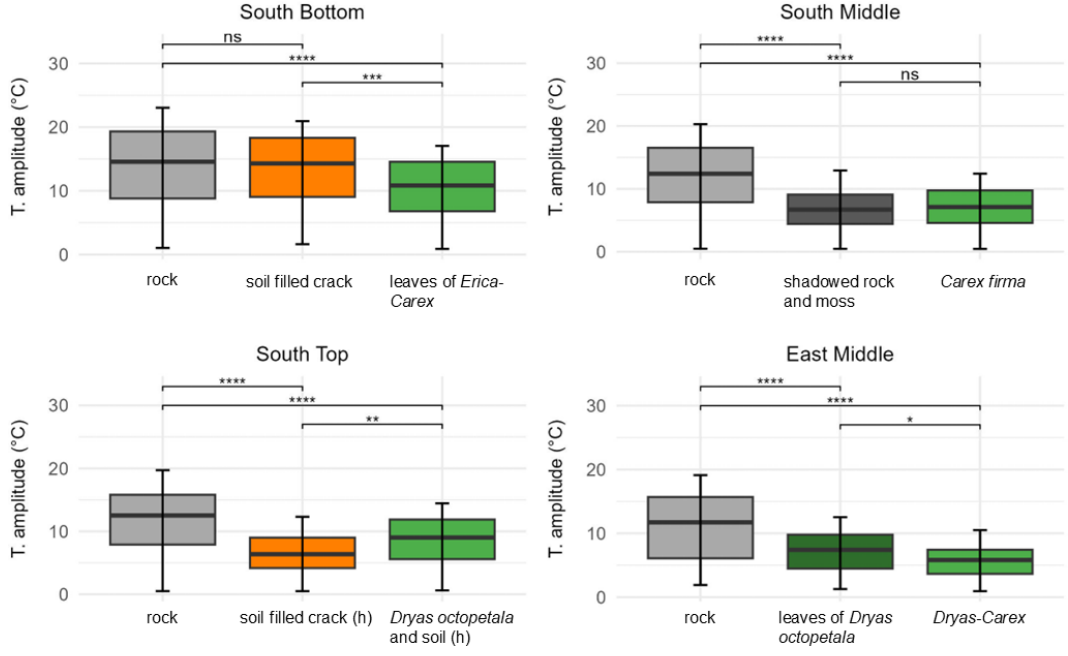

Figure 3. Distribution of the daily temperature amplitude in the rock with different cover at the surface from 27 May to 27 August (significance levels indicated by ns = not significant (p>0.05), * $p \leq 0.05$, ** $p \leq 0.01$, *** $p \leq 0.001$, **** $p \leq 0.0001$).

are in an intermediate position at ST and wettest at SB. This finding has to be treated with caution as the pore volume and structure of the rock in the vicinity of a crack can hardly be assessed. All discussed differences are statistically significant (Kruskal-Wallis p-value $< 2.2 \times 10^{16}$ for each site).

Electrical conductivity exhibits substantial temporal variability and displays distinct patterns for uncovered, soil covered, and vegetation covered rock (Fig. 5). At all sites, the conductivity of bare rock slightly decreases over the summer months which is in line with decreasing precipitation from June to August. The succession of phases of decreasing moisture (correlating with periods of dry weather) and sharply increasing moisture (correlating with rainfall events) can be found in a similar pattern at all sites. Notably, in a pronounced period of dry weather in the first half of August, a marked decrease in conductivity is evident across all sites.

At SB, conductivity fluctuations are almost identical between bare rock and vegetation cover (thin *Erica carnea* – *Carex firma*), as it was already found for the mean conductivity (Fig. 5). At SM, conductivity beneath shaded rock and moss cover displays the greatest range, surprisingly with higher maxima and deeper minima than at the bare rock site. *Carex firma* – covered rock exhibits similar maxima as the two rock sites but decreases much less in dry phases. At ST, uncovered rock has the lowest conductivity and the lowest fluctuations of all rock sites. In contrast, conductivity under

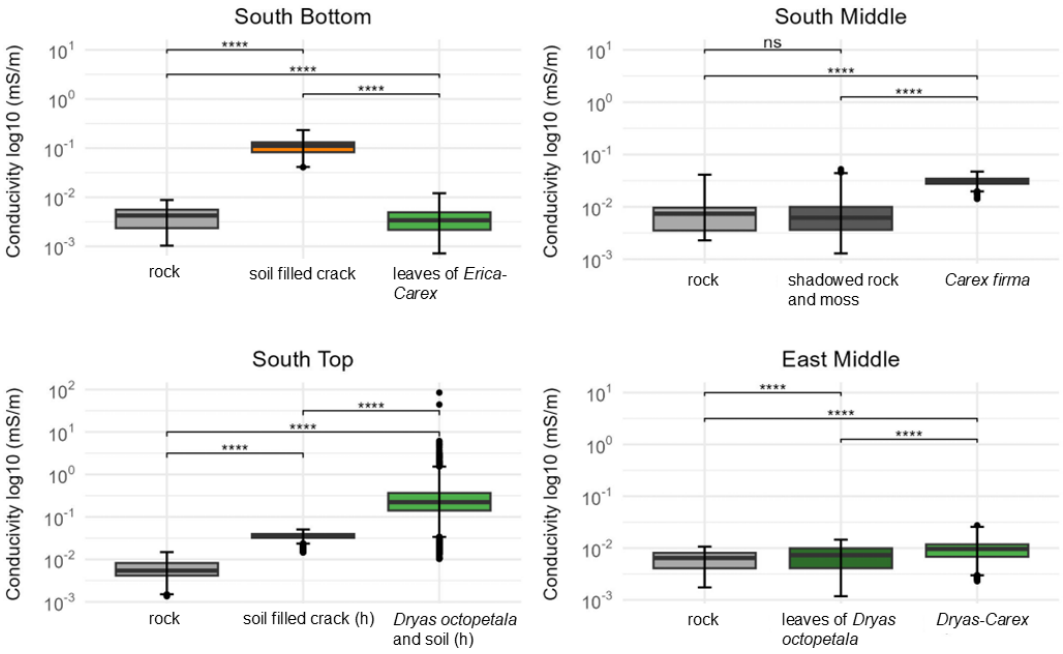

Figure 4. Distribution of the conductivity in the rock with different cover at the surface from 27 May to 27 August (significance levels indicated by ns = not significant ($p > 0.05$), **** $p \leq 0.0001$).

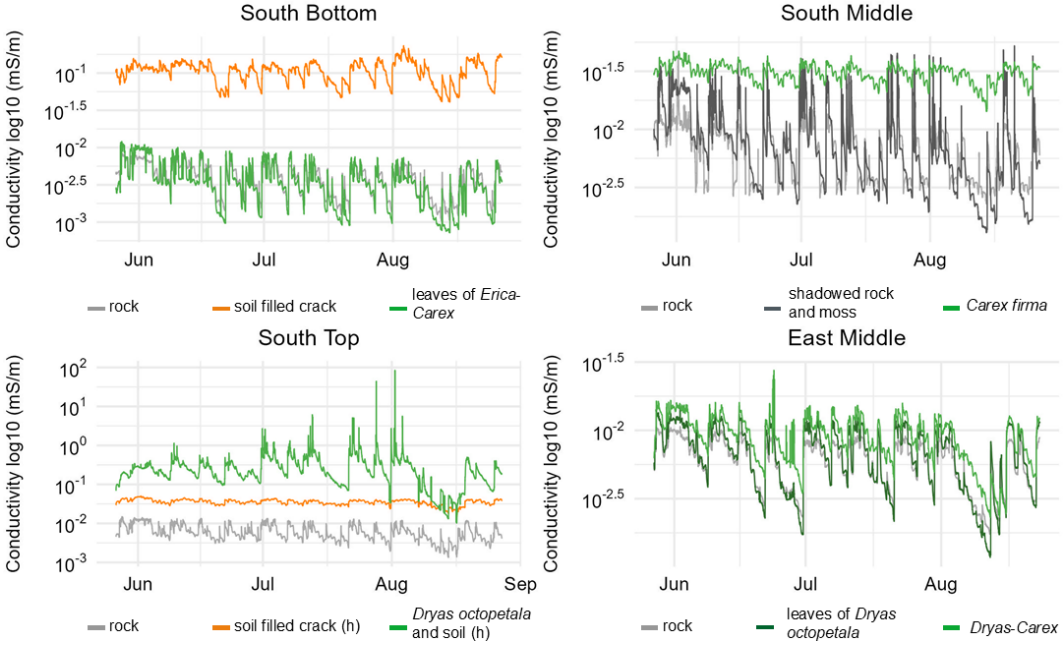

Figure 5. Development of the conductivity in the rock with different cover at the surface from 27 May to 27 August.

Dryas octopetala remains higher than beneath rock or soil, except for a brief decline in mid-August. Temporal fluctuations are pronounced, but minor wetting peaks (e.g. mid of July) observed at other sites appear to be buffered by the vegetation cover. The soil-filled crack maintains a consistent baseline with minimal fluctuations, presenting the most stable pattern among all measurement points. At EM, the temporal conductivity patterns below uncovered rock, *Dryas octopetala* and *Dryas-Carex* are almost identical in range and pattern. A remarkable difference between the two vegetation sites is the more pronounced drying under *Dryas octopetala* leaves (similar to bare rock) compared to *Dryas-Carex* cover.

The reaction on five exemplary distinct rain events (defined by a rainfall of ≥ 0.1 mm following dry periods of at least 24 h) in July 2024 are shown in Fig. 6. Events no. 1 and 3 were preceded by >24 h dry periods. The results show that the majority of sensor locations respond strongly to most rainfall events. However, the response varies in intensity at different locations and some rainfall events result in little or no response. While there was probably no sufficient drying time before the (weak) event 5, event 2 may have been very local. Due to recurring battery problems at EM there is a time lag between conductivity and rain events, which is why dates are not correct and rainfall events are not shown here.

Uncovered rock usually responds most quickly to rainfall, seen at all sites. The decline in conductivity is typically slow. For rock that is only covered by *Erica* and *Carex* leaves (SB) or by *Dryas* leaves (EM), conductivity also shows an immediate response to rainfall events. Conversely, measurement points with thick vegetation cover show a subdued and slightly delayed response (particularly *Carex firma* (SM) and *Dryas-Carex* complex (EM)); the drying between the events is also weaker here. At ST below *Dryas* and soil, the response to the first and second rain event is weak, but surprisingly fast and strong for events 3 and 4 which points to limited interception capacity during longer rainfall events. Soil-filled cracks (SB and ST) show a subdued reaction only to events 1 and 3; there is almost no reaction to events 2, 4 and 5 as the moisture decline in the shorter pre-rainfall periods is very weak. A remarkable detail is that at SM, shaded rock shows a considerably stronger reaction on the third and, particularly, fourth event. We attribute this to the observed occurrence of seepage water coming from a cleft at this point even after moderate rainfall.

4.4 Rock moisture: Small-scale distribution

The 2D-geoelectrical profiles were measured on 27 June. The weather was generally unstable in the preceding weeks, and during the day and night before there was occasional rainfall and high air humidity. The root mean square (RMS) error of the inverted 2D-resistivity sections was <10 % for the profiles ST, EL, and ER, 10 %–20 % at SB and SM and 29.5 % at EM. RMS < 10 % means a good fit considering the very heterogeneous conditions at small-scale rock sites and 10 %–30 % means still acceptable quality. Plant species, soil and cracks were added at the specific, measured locations on the profile.

The rock at SB is generally compact but showing deep cracks, which are often soil filled. The rock surface in between is not strongly fissured or weathered. The microrelief of the profile is relatively smooth. The most prominent feature in the ERT profile (Fig. 7) is the high conductivity near the surface at about 47–60 cm profile length with *Carex firma* and thin soil cover, and at about 67–80 cm with partly *Carex firma*, *Primula auricula* and soil cover. The depth of the moist "pockets" is about 5–10 cm at the first and about 10–15 cm at the second position. At 92–100 cm also with *Carex firma, Primula auricula* and soil cover, the conductivity is heightened but to a lesser degree and max. 5 cm deep, although *P. auricula* is an even larger individual there (Fig. 7). The sections with higher conductivity at 9, 21 and 31 cm profile length are remarkable, each corresponding to a soil-filled crack at the surface. Conversely, cracks with less soil cover around 45 and 65 cm profile length appear as low conductivity zones.

At East Middle, blueish colours (high moisture) are found at two prominent cracks in the middle of the profile (Fig. 8). Apart from these narrow zones, most of the surface is very dry, particularly under vegetation. The difference to ERT South Bottom (Fig. 7) is that the leave curtain of *Dryas octopetala* only covers the rock, keeping out direct rainfall without offering pits or rooting zones in which water could be stored. Due to high RMS error (29.5 %) resistivity distribution at greater depth is not interpreted.

The other four profiles can be characterized as follows (figures in the Supplement):

- South Middle: heightened conductivity under moss and under Carex firma, while no effect of a single *Primula auricula*
- South Top: high conductivity in the more shallow parts of the stepped profile, particularly under *Carex firma* + soil and under *Dryas octopetala*+soil; further wet spot under a patch of *Carex firma* and *Helianthemum alpestre*
- East left: heghtened conductivity around cracks and under rock areas shaded by *Rhododendron hirsutum*, as well as in mossy parts of the profile
- East right: heightened conductivity under vegetation filled fissures (*Carex firma*, *Rhododendron hirsutum* + soil), particularly under a combined patch of *Rhododendron hirsutum* and *Dryas octopetala*

For head R1M (depth range 0–3 cm), the average dimensionless moisture index (MI) varies from 524.2 (rock, SB) to 648.3 (*Carex firma*) and 648.5 (*Dryas octopetala*). The standard deviation ranges from 1.7 (*Rhododendron hirsutum*, EL2) to 103.0 (*C. firma*, SM-Logger). The MI value for 0–3 cm is generally lower for the uncovered rock than for the plant-covered rock (Fig. 9a). The difference at each study site from the respective uncovered rock reference value is greatest for *C. firma* with 86.5 MI units, followed by *D. octopetela* (79.8). The difference then decreases in the order of *Erica carnea* (60.7), *Globularia cordifolia* and *Rhododendron hirsutum* at EL2 (42.3), *Primula auricula* (35.3) and *Rhododendron hirsutum* at EL (31.4). Different species belonging to the same plant form (e.g. mat-forming chamaephytes) can have different responses, as seen for *D. octopetala* and *G. cordifolia* which do not share the same trend.

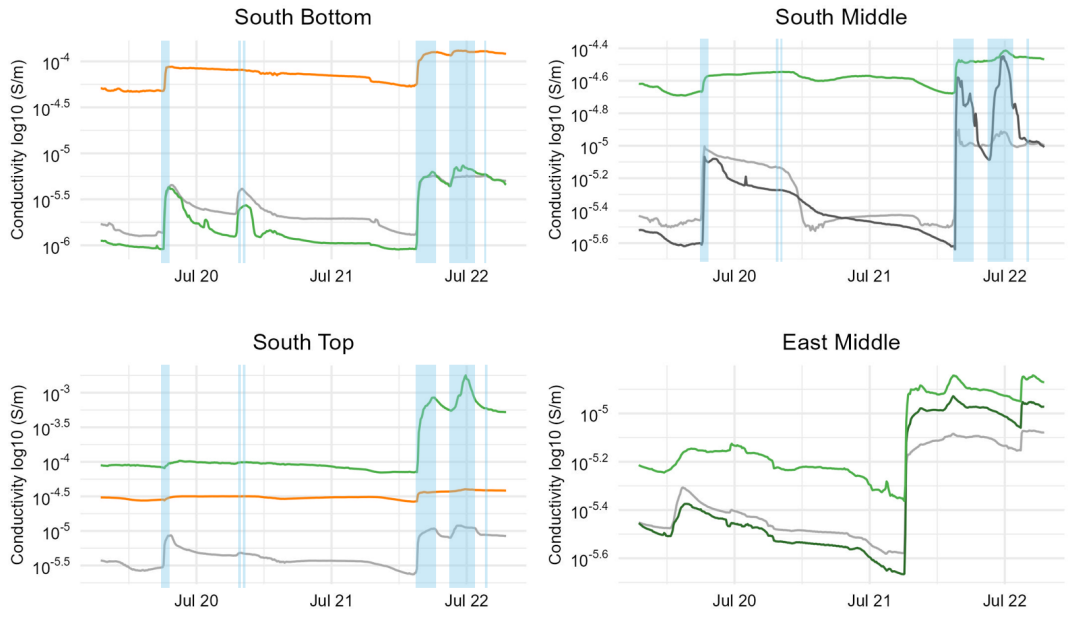

Figure 6. Response of conductivity in the rock on five rainfall events (19–22 July 2024) with different cover at the surface. At EM there is a time shift between rainfall and conductivity measurements due to logger malfunction which is why rainfall events are not shown.

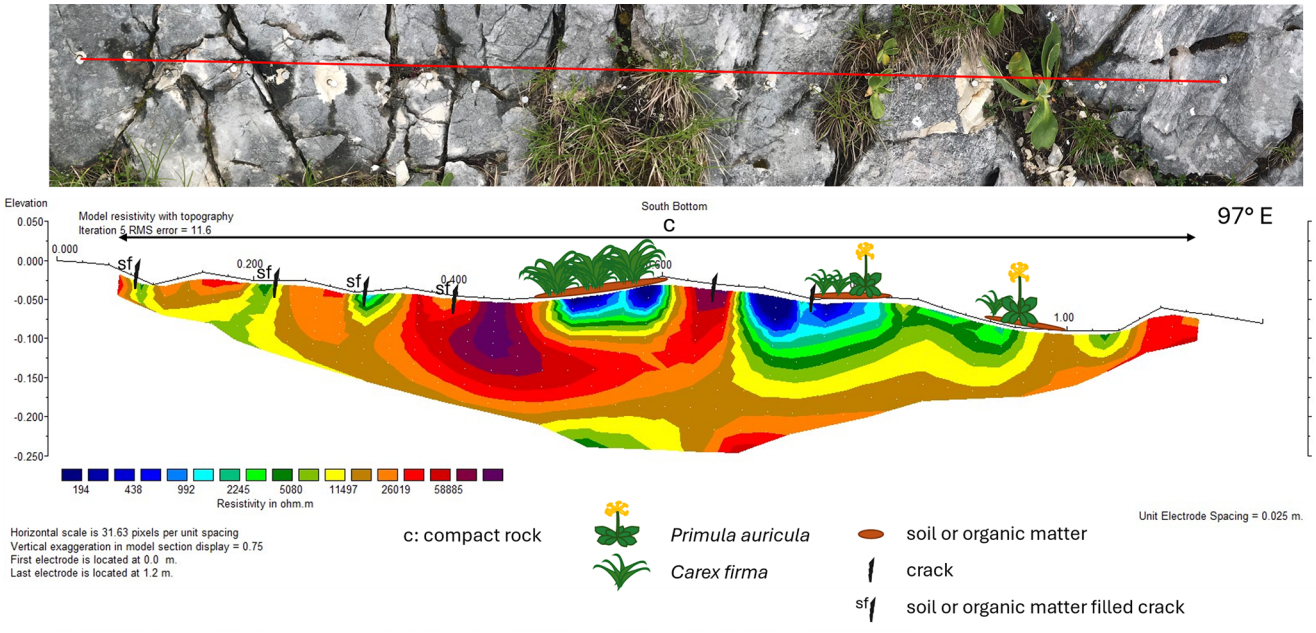

Figure 7. ERT profile at South Bottom (27 June 2024): Top: Photo of the profile (profile length 120 cm); Bottom: 2D-resistivity section, with blue colors representing low resistivity (high conductivity) and red colors high resistivity (low conductivity); complemented with information on cracks, soil and vegetation.

With head PM (0–25 cm), the average moisture index varies from 1926.7 (*Globularia cordifolia*) to 2210.0 (rock, EL) (Fig. 9b). The standard deviation is highest for *Rhododendron hirsutum* (EL) (147.4) and lowest for *Erica carnea* (30.3). The moisture index for 0–25 cm shows the reverse pattern for uncovered and covered rock, with uncovered rock mostly having higher values. Just below *Primula auricula*, the average MI is similar to rock. The largest difference in moisture index between plant-covered and uncovered rock occurs for *R. hirsutum* at EL (188.1 MI), followed by *G. cordifolia* (136.3), *E. carnea* (100.0), *R. hirsutum* (EL2) (52.7), *Carex firma* (43.2), *Dryas octopetala* (39.7) and fi-

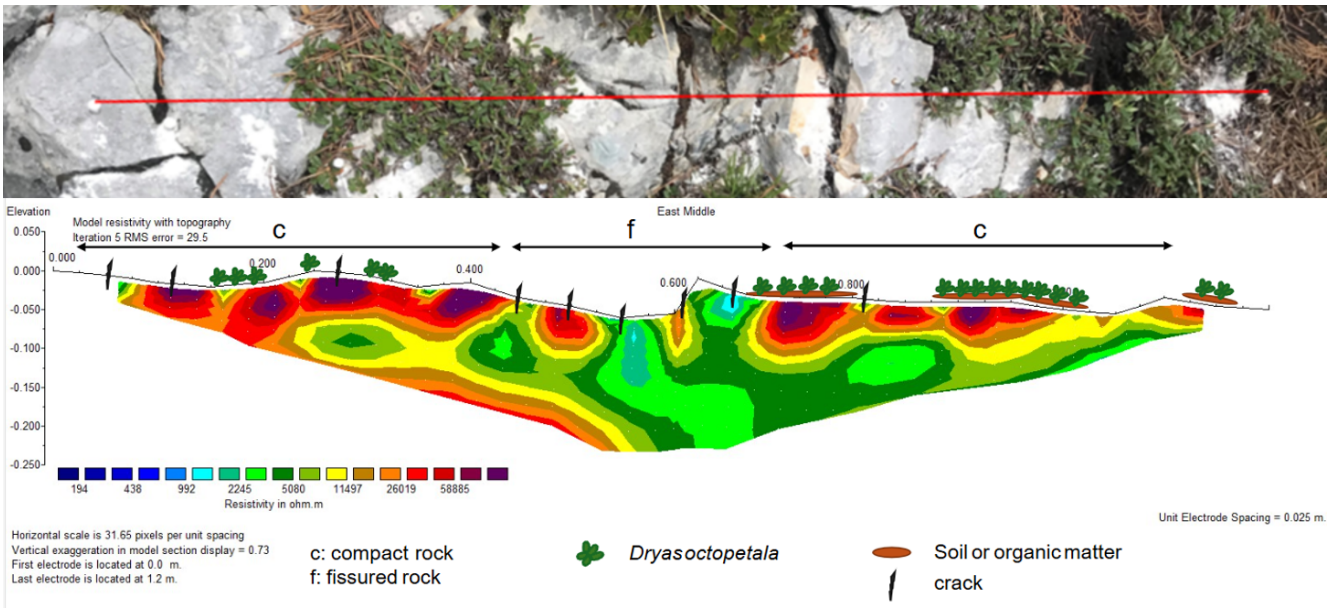

Figure 8. ERT profile at East Middle (27 June 2024): Top: Photo of the profile (distorted due to diagonal viewing angle); Bottom: 2D-resistivity section, with blue colors representing low resistivity (high conductivity) and red colors high resistivity (low conductivity); complemented with information on cracks, soil and vegetation.

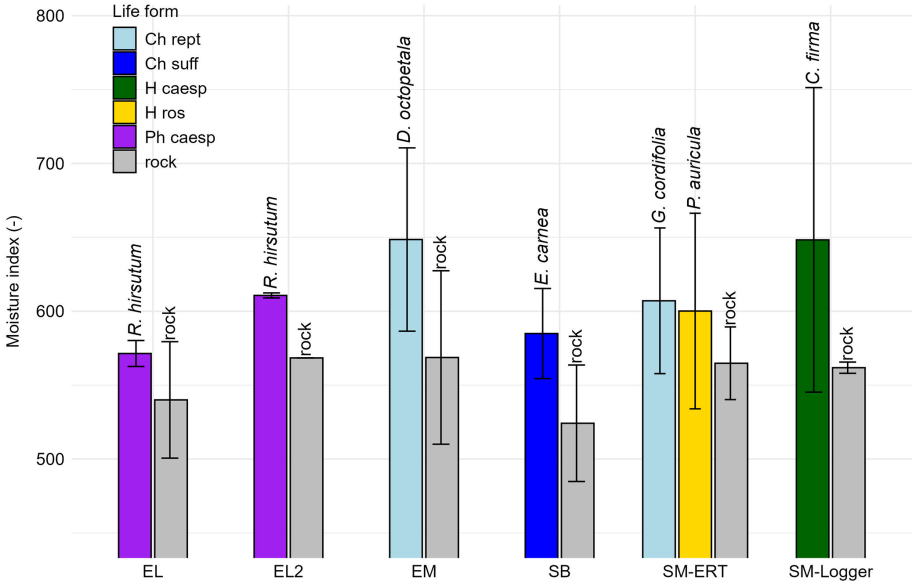

Figure 9. Dimensionless MW moisture index with cover of different plant species; 0–3 cm rock depth (plant forms according to Ellenberg and Mueller-Dombois (1967): Ch rept = mat-forming chamaephyte, Ch suff = subshrubby chamaephyte, H caesp = tufted hemicryptophyte, H ros = rosette hemicryptophyte, Ph caesp = tufted phanerophyte).

nally *P. auricula* (5.3). Again, no shared trend can be seen for *D. octopetala* and *G. cordifolia* within the plant form of mat-forming chamaephytes (Fig. 10). No data on rooting depth were available in TRY for our species pool.

5 Discussion

The novel combination of three different techniques of small-scale rock temperature and rock moisture measurement proved to be a promising approach for characterising the potential impact of different plant species on rock microclimate and weathering. The dataset is consistent, with the

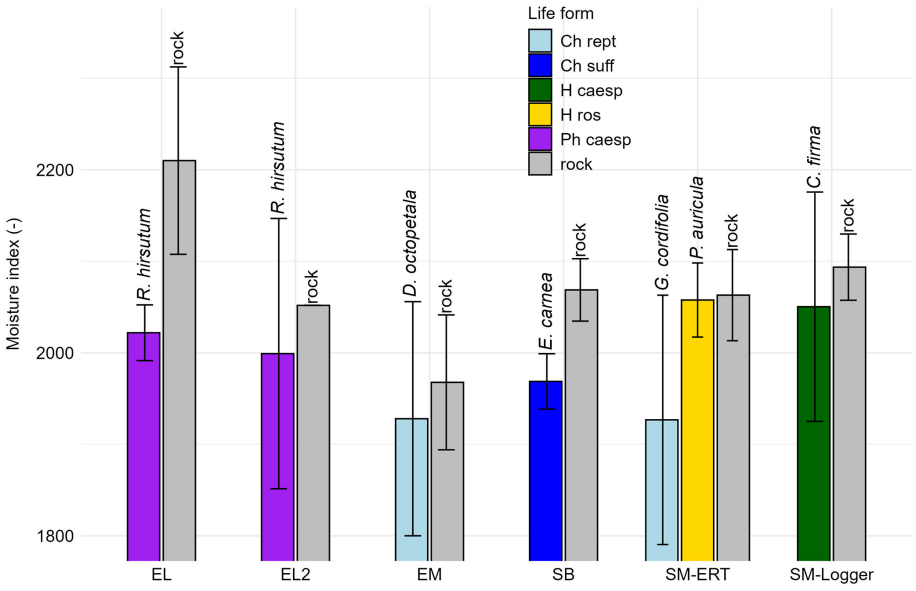

Figure 10. Dimensionless MW moisture index with cover of different plant species; 0–25 cm rock depth (life forms see Fig. 9).

three techniques (T/ER logger, ERT, MW) yielding different types of information. For all three techniques, absolute calibration (to e.g volumetric moisture content) is difficult as samples used in the laboratory differ from the complex conditions (especially joints) encountered in the field. Empiric calibration in the field (by observing minima in long dry periods and maxima after long wet periods) is a more promising approach than calibration using samples in the lab; with longer measurement periods, we will be able to determine the possible value range. For the moment, higher/lower conductivity and microwave values are interpreted as "wetter" and "drier", respectively.

The daily rock temperature amplitude is consistently reduced with vegetation across all sites. The attenuation is 3.2–5.2 K compared to uncovered rock. The difference tends to be greater under plant/soil complexes (*D. octopetala* or *C. firma*) compared to the effects of just leaves. However, pronounced individual differences between micro-sites have to be considered. Similar attenuation of rate and amplitude of daily temperature cycles by vegetation in the growing season was also observed by Gage et al. (2024) at the Niagara escarpment. As the amplitude of daily temperature fluctuations is a key factor in thermal stresses (Hall and Thorn, 2014; Ravaji et al., 2019; Ito et al., 2021) there is no doubt that the thermal attenuation by vegetation in our study area reduces thermal stresses. This is also supported by the considerable reduction in the rate of temperature change.

Although there were no subzero temperatures in our measurement period as we did not measure in winter, we assume that the number of freeze-thaw cycles will be reduced by vegetation and soil. It is very likely that the same attenuation of temperature will occur during winter months as most of the investigated species are evergreen. Temperature patterns in winter can be modified by snow cover which is, however, relatively short at the exposed sites of our study area. Currently we cannot estimate if annual minima during long-lasting freezing periods or the time spent in the frost-cracking window (Hallet et al., 1991; Murton et al. 2006; Mayer et al., 2023) will also be affected. Continuing measurements will clarify this point in the future.

Moisture in the rock increases with vegetation and soil cover, with a predominant effect induced by the presence of soil. The results suggest that in general plants and soil increase the humidity in the rock. The presence of soil, with or without the presence of plants, seems to be a necessary condition to create situations with a conductivity at least one order of magnitude higher than bare rock. The presence of leaf canopy alone does not have a clear effect. Results obtained with the microwave measurements suggest that plants in their integrity as overall organisms help retain moisture near the rock surface (0–3 cm) by shading the surface and by producing and trapping litter and organic matter, while causing drying at greater depths (0–25 cm) by their interception at leaves and branches and by their evapotranspiration. Moisture in the ERT profiles confirms this interpretation as it is heightened in the plant's rooting zone but lower under leaf cover (e.g., ERT profile EM under *Dryas octopetala*). Increases in humidity and the presence of liquid water lead to exponential acceleration of subcritical cracking (Eppes and Keanini, 2017; Eppes et al., 2020). Thus, a potentially enhancing effect on rock decay along soil- or root-filled clefts is very probable. Furthermore, laboratory investigation of rocks using acoustic emission sensors show that samples with high saturation subjected to freeze-thaw cycles produce many more acoustic signals (indicating crack formation) than dry samples (Mitchell and Sass, 2024), which means that water retention by plants

potentially intensifies frost weathering. At present, it is uncertain whether the dampening effect of temperature or the intensifying effect of humidity has a greater overall impact.

Results show that changes in rock moisture are in fact dominated by rain events. The impact of melting snow will be evaluated in a follow-up study. Uncovered rock usually responds most quickly to rainfall, while measurement points with soil or vegetation cover show a subdued and slightly delayed response, which we mainly assign to leaf interception. On the other hand, moisture from rainfall events is retained longer at vegetation- and soil-covered sites. The consequences for weathering are equivocal. Quick moisture fluctuations on bare rock might contribute to rock decay (e.g. Yang et al., 2018; Dong et al., 2023) while longer dry periods might reduce weathering. Prolonged deep wetting of stone may facilitate the movement of salts or organic acids deep into micro cracks, thus promoting chemical weathering (McAllister et al., 2017).

The detected variations between life forms and species suggest that these play distinct roles. Tufted and mat-forming species retain moisture near the rock surface (0–3 cm) more effectively than subshrubby or rosette species, suggesting that this effect is driven by the architecture of aboveground organs, as we hypothesized. Unique species-specific impacts also emerge. The reduced moisture retention observed near the rock surface (0–3 cm) in *Primula auricula* may be due to the fact that this rosette species has leaves that are not pressed against the ground. Furthermore, this species exhibits an almost negligible effect on moisture at greater depths (0–25 cm), suggesting a relatively shallow root system, which is consistent with observations that its taproot is partially exposed in cracks (Murray, 1934). At greater depths in the rock (0–25 cm), distinctions between life forms become apparent, in agreement with Nie et al. (2019). In our study, chamaephytes and phanerophytes tend to exploit water deeper in the rock than hemicryptophytes. This observed pattern partially aligns with the correspondence between above- and belowground plant sizes (Beccari and Carmona, 2024), with larger species (*Rhododendron hirsutum* and *Erica carnea*) able to access water resources at greater depths compared to smaller species (*Carex firma* and *Primula auricula*). In addition, non-clonal species with a single main root axis, such as *Primula auricula*, are more likely to encounter impenetrable rock that hinders root expansion, thereby forcing them to rely on superficial water sources. In contrast, branched root systems enhance the ability to access water stored in fissures through coarse roots (Poot et al., 2012), and to forage at greater depths. The lack of available rooting depth data for our species pool prevented us from directly testing these patterns.

The process of biological weathering induced by vascular plants does not occur homogeneously on the rock surface. At the steep slopes of our study site, vascular plants primarily establish themselves in microtopographic features such as pockets, ledges, and cracks in the rock (Kuntz and Larson, 2006). Just with their lateral growth, the roots do not exert sufficient pressure on the surrounding rock to cause dense and massive rock to crack (Malik et al., 2019). However, through their presence, vascular plants contribute to the physical alteration of these microenvironments and the immediately surrounding space by accumulating organic matter and litter, locally modifying hydrology through evapotranspiration, intercepting part of the precipitation, and shielding the underlying rock from short-wave radiation with their aboveground organs. The magnitude of these effects depends on species identity, encompassing variation in growth form, life form, and root architecture. While our study is geographically constrained, the results may be extended beyond the study area. First, most of the selected species have distribution ranges spanning southern European mountain systems (except *Rhododendron hirsutum*, restricted to the Alps) and represent different Raunkiaer life forms (e.g. chamaephytes, hemicryptophytes), which are widely reported across rocky outcrop systems on carbonate substrates beyond the distribution ranges of the studied taxa (Larson et al., 2000; Raevel et al., 2013). Second, the species exhibit contrasting growth forms (e.g. reptant, caespitose, rosulate) and root architectures, thereby capturing a range of plant–substrate interaction strategies that may occur across different rocky habitats. These physical alterations are expected to influence weathering rates, increasing them due to higher moisture within the root system while simultaneously reducing them due to a decreased amplitude of surface temperature and moisture under the leaves. Which of these effects prevails cannot be answered yet from our preliminary study.

Vascular plant communities could therefore have both a stabilizing function for the substrate in which they persist or a destabilizing one for the rocks. This has interesting implications not only for defining weathering rates but also for understanding the dynamics of these plant communities. Bemis et al. (2026) ask the question: "Does vegetation colonize areas of favorable existing regolith, or does vegetation create a regolith that suits its needs?" On the steep slopes of our study site the answer is clear: Our investigated species root in cracks of the rock where they are able to influence weathering, while sites with more loose debris are home to a set of entirely different plant species with different root architecture. On mobile slope regolith plant roots are specifically adapted to stabilise scree, not to penetrate crevices. If rock plants generate significant amounts of regolith, they pave the way for other species, not for their own needs.

6 Conclusions

Temperature measurements, 1D- and 2D-resistivity and microwave techniques offer promising opportunities to assess how alpine plants mediate microclimate and rock weathering. The results provide insights into how species explore water resources in rocky substrates, providing a potential tool

to estimate root depth in environments that are particularly difficult to sample.

The results show that diurnal temperature cycles and change rates are attenuated under plant roots and leaves, potentially reducing the efficacy of thermal and frost cracking. Water is retained and stored by plants, causing pockets of wet substrate under plant roots and soil (particularly under *Carex firma* and *Dryas octopetala*) while a pure leaf curtain on the rock has a much lower or reverse effect. Microwave measurements indicate that plants increase moisture in the uppermost centimetres of rock while at greater depth, rock beneath plants is drier (probably due to interception loss and transpiration). Higher and deeper-seated moisture has the potential to promote subcritical cracking. There are variations between different species and functional types, likely driven by differences in the architecture of both above- and below-ground organs.

The results underline a biogeomorphological co-evolution at alpine rocky sites, with weathering providing micro-sites for plants and plants mediating rock weathering.

Appendix A

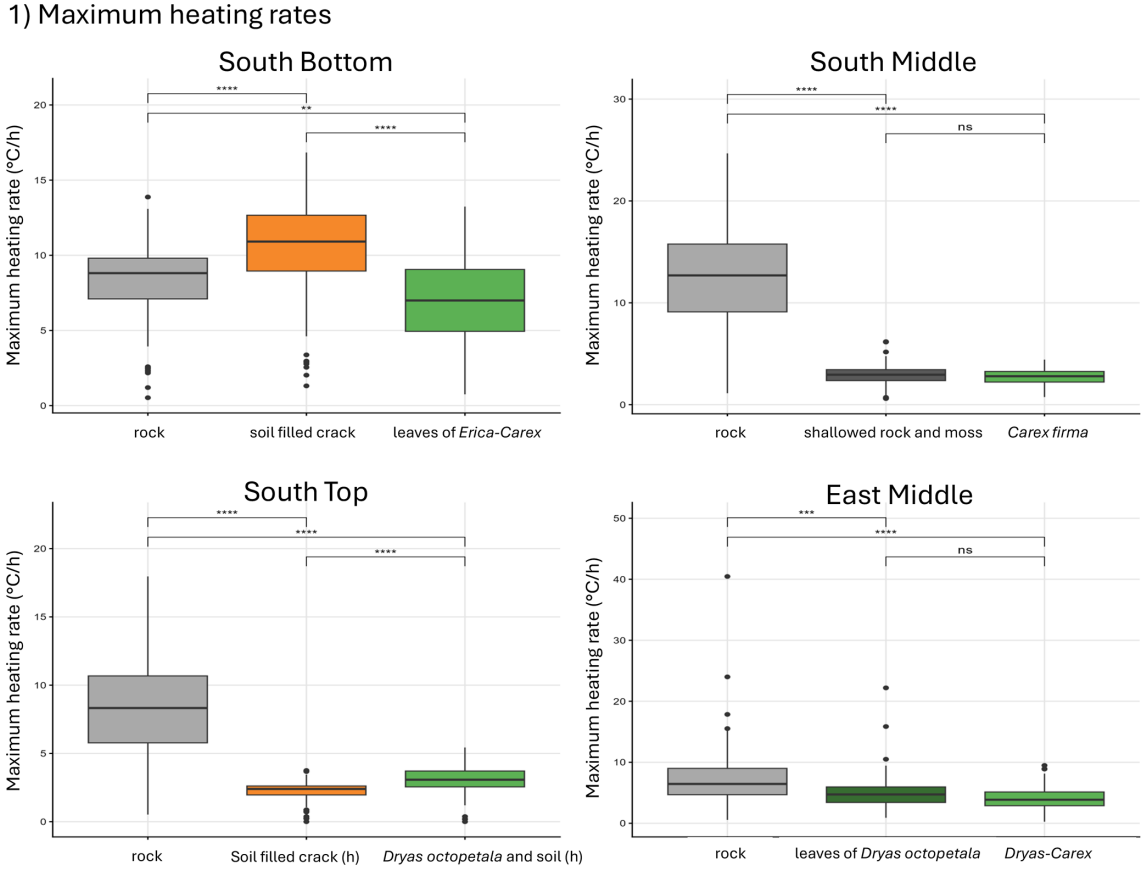

Figure A1.

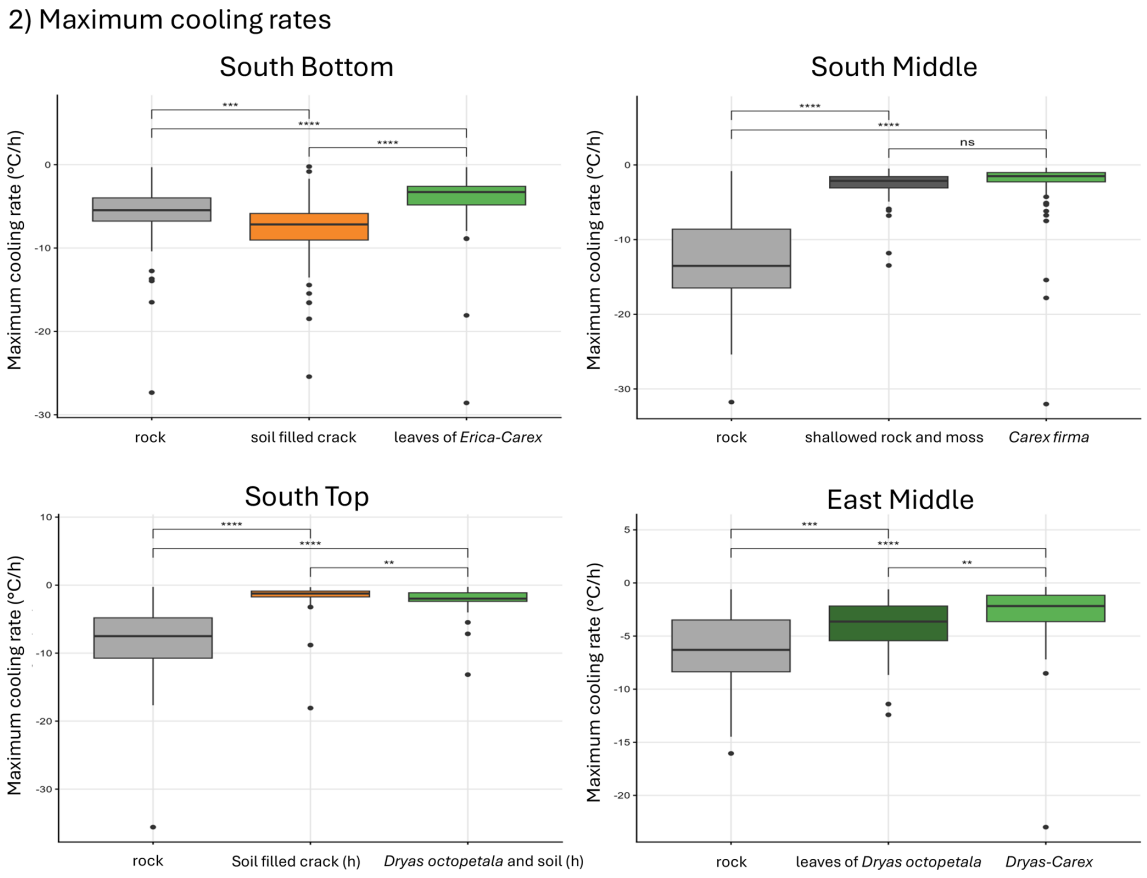

Figure A1. Maximum heating and cooling rates in the rock with different cover at the surface from 27 May to 27 August (significance levels indicated by ns = not significant (p>0.05), * $p \leq 0.05$, ** $p \leq 0.01$, *** $p \leq 0.001$, **** $p \leq 0.0001$). Temperature change rates are systematically higher in bare rock compared to vegetation cover. The noteable exception of South Bottom/soil filled crack is thought to be caused by lower albedo of dark soil or lower heat capacity of dry soil compared to rock.

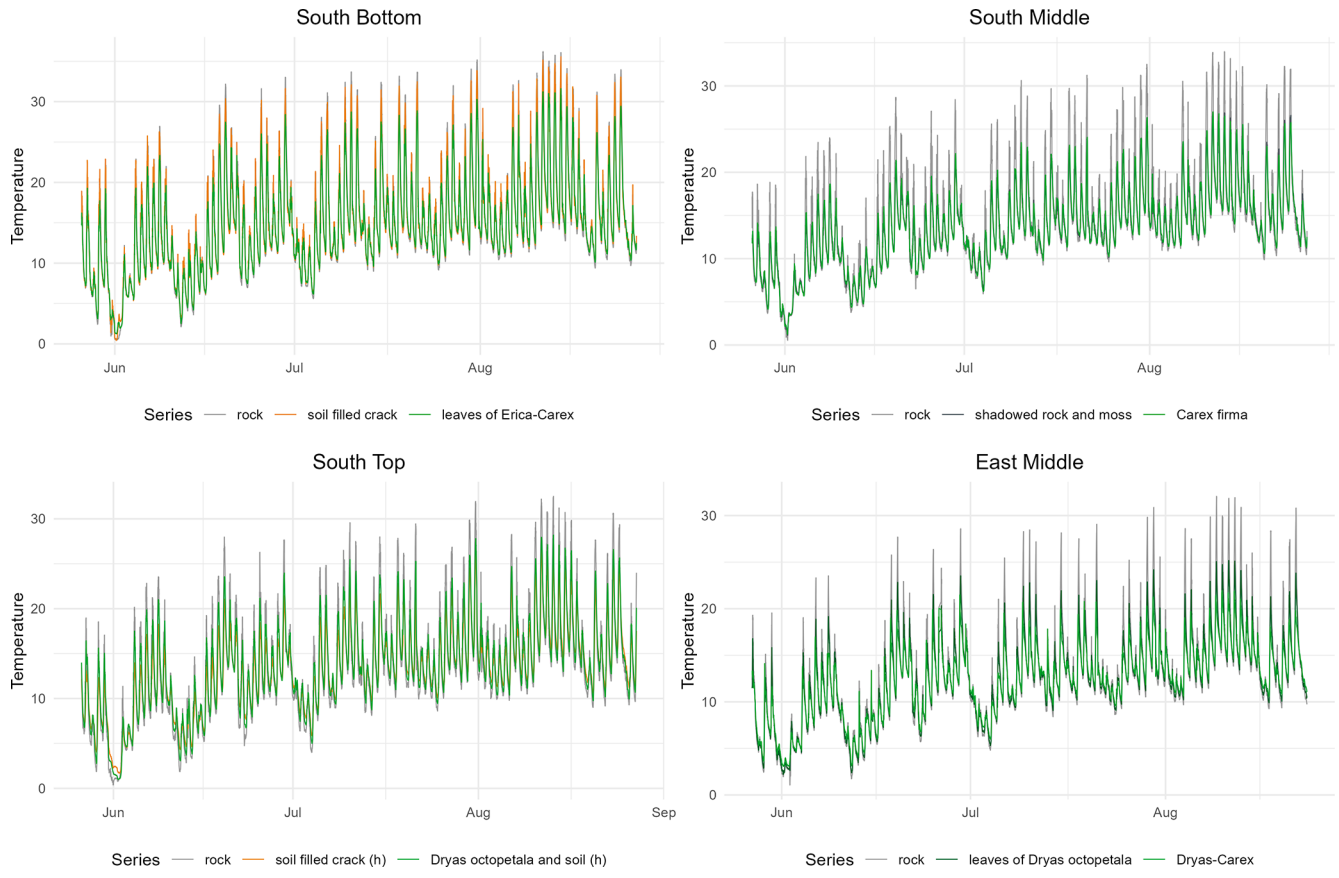

Figure A2. Development of the temperature in the rock with different cover at the surface from 27 May to 27 August.

Data availability. We provided unrestricted access to all data and materials underlying reported findings; namely temperature and conductivity logger data, ERT raw files and microwave sensor data. These are available at https://doi.org/10.5281/zenodo.17768495 (Sass et al., 2025).

Author contributions. OS conceptualized the methodology and research plan from the geomorphology and rock moisture side and AJ from the disturbance ecology side; both provided funding and resources. UB carried out the field and lab investigation and wrote a MSc thesis on the topic. In the entire process, UB was supervised by OS from the geomorphology and rock moisture side and TD from the disturbance ecology side. At UB's request, OS took the lead in original draft preparation and wrote large parts of the text. TD contributed for the writing of the disturbance ecology side. TD and AJ contributed with review and editing.

Competing interests. The contact author has declared that none of the authors has any competing interests.

Disclaimer. Publisher's note: Copernicus Publications remains neutral with regard to jurisdictional claims made in the text, published maps, institutional affiliations, or any other geographical representation in this paper. The authors bear the ultimate responsibility for providing appropriate place names. Views expressed in the text are those of the authors and do not necessarily reflect the views of the publisher.

Acknowledgements. We are grateful for the constructive comments from Missy Eppes and a second anonymous reviewer. We would like to thank Andrew Mitchell and Manfred Fischer for their help in the geomorphology lab. Sincere thanks to Elisabeth Burger for her voluntary assistance with the fieldwork.

Financial support. The work, being a pre-study for a planned project application, was carried out using internal funds (Chairs of Geomorphology and of Disturbance Ecology, University of Bayreuth).

Review statement. This paper was edited by David Medvigy and reviewed by Martha-Cary Eppes and one anonymous referee.

References

Aalto, J., Le Roux, P. C., and Luoto, M.: Vegetation mediates soil temperature and moisture in arctic-alpine environments, Arct. Antarct. Alp. Res., 45, 429–439, https://doi.org/10.1657/1938-4246-45.4.429, 2013.

Algeo, T. J., Berner, R. A., Maynard, J. B., and Scheckler, S. E.: Late Devonian oceanic anoxic events and biotic crises: "rooted" in the evolution of vascular land plants, GSA today, 5, 64–66, https://www.researchgate.net/publication/230891610_Late_Devonian_oceanic_anoxic_events_and_biotic_crises_Rooted_in_the_evolution_of_vascular_plants (last access: 12 May 2026), 1995.

Beccari, E. and Carmona, C. P.: Aboveground and belowground sizes are aligned in the unified spectrum of plant form and function, Nat. Commun., 15, 9199, https://doi.org/10.1038/s41467-024-53180-x, 2024.

Bemis, S. P., Holbrook, W. S., Flinchum, B., Hayes, J., Callahan, R., Harman, C., Carr, B., and Riebe, C.: Creating a critical zone: Feedbacks between bedrock geology, water retention, and vegetation on an exposed bedrock surface, Panola Mountain, Georgia, USA, J. Geophys. Res.-Earth, 131, e2025JF008424, https://doi.org/10.1029/2025JF008424, 2026.

Calabrese, S. and Porporato, A.: Wetness controls on global chemical weathering, Envir. Res. Commun., 2, 085005, https://doi.org/10.1088/2515-7620/abad7b, 2020.

Coombes, M. A., Viles, H. A., and Zhang, H.: Thermal blanketing by ivy (Hedera helix L.) can protect building stone from damaging frosts, Sci. Rep., 8, 9834, https://doi.org/10.1038/s41598-018-28276-2, 2018.

Corenblit, D., Baas, A. C., Bornette, G., Darrozes, J., Delmotte, S., Francis, R. A., Gurnell, A. M., Julien, F., Naiman, R. J., and Steiger, J.: Feedbacks between geomorphology and biota controlling Earth surface processes and landforms: a review of foundation concepts and current understandings, Earth-Sci. Rev., 106, 307–331, https://doi.org/10.1016/j.earscirev.2011.03.002, 2011.

Dahanayake, A. C., Webb, J. A., Greet, J., and Brookes, J. D.: How do plants reduce erosion? An Eco Evidence assessment, Plant Ecol., 225, 593–604, https://doi.org/10.1007/s11258-024-01414-9, 2024.

Dahlin, T.: 2D resistivity surveying for environmental and engineering applications, First break, 14, https://doi.org/10.3997/1365-2397.1996007, 1996.

D'Alvia, L., Pittella, E., Rizzuto, E., Piuzzi, E., and Del Prete, Z.: A portable low-cost reflectometric setup for moisture measurement in cultural heritage masonry unit, Measurement, 189, 110438, https://doi.org/10.1016/j.measurement.2021.110438, 2022.

De Giuli, M., Winkler, M., Deola, T., Henschel, J., Sass, O., Wolff, P., and Jentsch, A.: Arrested succession on fire-affected slopes in the Krummholz zone and subalpine forest of the northern limestone alps, Diversity, 16, 366, https://doi.org/10.3390/d16070366, 2024.

De Groeve, M., Kale, E., Godts, S., Orr, S. A., and De Kock, T.: Impact of vertical greening on urban microclimate and historic building materials: A meta-analysis, Build. Environ., 253, 111365, https://doi.org/10.1016/j.buildenv.2024.111365, 2024.

Deprez, M., De Kock, T., De Schutter, G., and Cnudde, V.: A review on freeze-thaw action and weathering of rocks, Earth-Sci. Rev., 203, 103143, https://doi.org/10.1016/j.earscirev.2020.103143, 2020.

Derry, L. A.: Weathering and climate, in: Encyclopedia of Paleoclimatology and Ancient Environments, Springer, Dordrecht, 981–986, https://doi.org/10.1007/978-1-4020-4411-3_217, 2009.

Dong, Q., Sun, X., Lei, N., and Liu, B.: Effect of dry–wet cycling on the degradation characteristics and mechanisms of red sandstone, Geofluids, 2023, 9950331, https://doi.org/10.1155/2023/9950331, 2023.

Draebing, D. and Mayer, T.: Topographic and geologic controls on frost cracking in Alpine rockwalls, J. Geophys. Res.-Earth, 126, e2021JF006163, https://doi.org/10.1029/2021JF006163, 2021.

Eichel, J., Corenblit, D., and Dikau, R.: Conditions for feedbacks between geomorphic and vegetation dynamics on lateral moraine slopes: a biogeomorphic feedback window, Earth Surf. Process. Landf., 41, 406–419, https://doi.org/10.1002/esp.3859, 2016.

Ellenberg, H. and Mueller-Dombois, D.: A key to Raunkiaer plant life forms with revised subdivisions, https://www.researchgate.net/publication/267393597_A_Key_to_Raunkiaer_plant_life_forms_with_revised_subdivisions (last access: 12 May 2026), 1967.

Eppes, M. C. and Keanini, R.: Mechanical weathering and rock erosion by climate-dependent subcritical cracking, Rev. Geophys., 55, 470–508, https://doi.org/10.1002/2017RG000557, 2017.

Eppes, M. C., Magi, B., Scheff, J., Warren, K., Ching, S., and Feng, T.: Warmer, wetter climates accelerate mechanical weathering in field data, independent of stress-loading, Geophys. Res. Lett., 47, 2020GL089062, https://doi.org/10.1029/2020GL089062, 2020.

Gage, H. J., Nielsen, J. P., and Eyles, C. H.: Temporal variability and site specificity of thermomechanical weathering in a temperate climate, Front. Earth Sci., 12, 1318747, https://doi.org/10.3389/feart.2024.1318747, 2024.

Gaylarde, C.: Influence of environment on microbial colonization of historic stone buildings with emphasis on cyanobacteria, Heritage, 3, 1469–1482, https://doi.org/10.3390/heritage3040080, 2020.

Godts, S., Orr, S. A., Steiger, M., Stahlbuhk, A., De Kock, T., Desarnaud, J., De Clercq, H., and Cnudde, V: Salt mixtures in stone weathering, Sci. Rep., 13, 13306, https://doi.org/10.1038/s41598-023-40590-y, 2023.

Hales, T. C. and Roering, J. J.: Climatic controls on frost cracking and implications for the evolution of bedrock landscapes, J. Geophys. Res.-Earth, 112, https://doi.org/10.1029/2006JF000616, 2007.

Hall, K.: The role of thermal stress fatigue in the breakdown of rock in cold regions, Geomorphology, 31, 47–63, https://doi.org/10.1016/S0169-555X(99)00072-0, 1999.

Hall, K. and Thorn, C. E.: Thermal fatigue and thermal shock in bedrock: An attempt to unravel the geomorphic processes and products, Geomorphology, 206, 1–13, https://doi.org/10.1016/j.geomorph.2013.09.013, 2014.

Hallet, B., Walder, J. S., and Stubbs, C. W.: Weathering by segregation ice growth in microcracks at sustained subzero temperatures: Verification from an experimental study using acoustic emissions, Permafrost Periglac. Process., 2, 283–300, https://doi.org/10.1002/ppp.3430020404, 1991.

Hassler, M. and Muer, T.: Flora Germanica: alle Farn- und Blütenpflanzen Deutschlands in Text und Bild, Verlag Regionalkultur, Überstadt-Weiher, ISBN 978-3-95505-482-3, 2022.

Hayashi, M.: Temperature-electrical conductivity relation of water for environmental monitoring and geophysi-

cal data inversion, Environ. Monit. Assess., 96, 119–128, https://doi.org/10.1023/B:EMAS.0000031719.83065.68, 2004.

He, S., Zhang, C., Meng, F. R., Bourque, C. P. A., Huang, Z., Li, X., Han, Y., Feng, S., Miao, L., and Liu, C.: Vegetation-cover control of between-site soil temperature evolution in a sandy desertland, Sci. Total Environ., 908, 168372, https://doi.org/10.1016/j.scitotenv.2023.168372, 2024.

InfoFlora: Das nationale Daten- und Informationszentrum der Schweizer Flora, infoflora, https://www.infoflora.ch/de/ (last access: 26 December 2024), 2024.

Ito, W. H., Scussiato, T., Vagnon, F., Ferrero, A. M., Migliazza, M. R., Ramis, J., and de Queiroz, P. I. B.: On the thermal stresses due to weathering in natural stones, Appl. Sci., 11, 1188, https://doi.org/10.3390/app11031188, 2021.

Jackson, G. and Sheldon, J.: The vegetation of magnesian limestone cliffs at Markland Grips near Sheffield, J. Ecol., 38–50, https://www.jstor.org/stable/2256729 (last access: 12 May 2026), 1949.

Kattge, J., Bönisch, G., Díaz, S., et al.: TRY plant trait database – enhanced coverage and open access, Glob. Change Biol., 26, 119–188, https://doi.org/10.1111/gcb.14904, 2020.

Klamerus-Iwan, A., Link, T. E., Keim, R. F., and Van Stan II, J. T.: Storage and routing of precipitation through canopies, in: Precipitation partitioning by vegetation: A global synthesis, Springer International Publishing, Cham, 17–34, https://doi.org/10.1007/978-3-030-29702-2_2, 2020.

Klimešová, J. and Klimeš, L.: Clo-Pla3 – database of clonal growth of plants from Central Europe, http://clopla.butbn.cas.cz/ (last access: 1 September 2025), 2024.

Körner, C.: Alpine Plant Life. Functional Plant Ecology of High Mountain Ecosystems, 3rd edn., Springer Nature Switzerland AG, https://doi.org/10.1007/978-3-030-59538-8, 2021.

Kuntz, K. L. and Larson, D. W.: Microtopographic control of vascular plant, bryophyte and lichen communities on cliff faces, Plant Ecol., 185, 239–253, https://doi.org/10.1007/s11258-006-9101-z, 2006.

Kutschera, L. and Lichtenegger, E.: Wurzelatlas mitteleuropäischer Grünlandpflanzen, Gustav Fischer Verlag, Stuttgart, New York, https://images.wur.nl/digital/collection/coll13 (last access: 12 May 2026), 1982.

Kutschera, L. and Lichtenegger, E.: Wurzelatlas mitteleuropäischer Grünlandpflanzen, Gustav Fischer Verlag, Stuttgart, Jena, New York, https://images.wur.nl/digital/collection/coll13 (last access: 12 May 2026), 1992.

Kutschera, L., Sobotik, M., and Lichtenegger, E.: Bewurzelung von Pflanzen in den verschiedenen Lebensräumen, Linz: Oberösterreichisches Landesmuseum, Bd. 5, https://images.wur.nl/digital/collection/coll13 (last access: 12 May 2026), 1997.

Larsen, I. J., Eger, A., Almond, P. C., Thaler, E. A., Rhodes, J. M., and Prasicek, G.: The influence of erosion and vegetation on soil production and chemical weathering rates in the Southern Alps, New Zealand, Earth Planet. Sci. Lett., 608, 118036, https://doi.org/10.1016/j.epsl.2023.118036, 2023.

Larson, D. W., Matthes, U., and Kelly, P. E.: Cliff ecology: pattern and process in cliff ecosystems, Cambridge University Press, Cambridge, ISBN-13 978-0-521-55489-3, 2000.

Leucci, G., Cataldo, R., and De Nunzio, G.: Assessment of fractures in some columns inside the crypt of the Cattedrale di Otranto using integrated geophysical methods, J. Archaeol. Sci., 34, 222–232, https://doi.org/10.1016/j.jas.2006.05.008, 2007.

Liu, H., Dai, J., Xu, C., Peng, J., Wu, X., and Wang, H.: Bedrock-associated belowground and aboveground interactions and their implications for vegetation restoration in the karst critical zone of subtropical Southwest China, Prog. Phys. Geogr: Earth Environ., 45, 7–19, https://doi.org/10.1177/0309133320949865, 2021.

Loke, M. H.: Electrical imaging surveys for environmental and engineering studies. A practical guide to, 2, 70, https://pages.mtu.edu/~ctyoung/LOKENOTE.PDF (last access: 12 May 2026), 1999.

Malik, I., Pawlik, Ł., Ślęzak, A., and Wistuba, M.: A study of the wood anatomy of Picea abies roots and their role in biomechanical weathering of rock cracks, Catena, 173, 264–275, 2019.

Marston, R. A.: Geomorphology and vegetation on hillslopes: Interactions, dependencies, and feedback loops, Geomorphology, 116, 206–217, https://doi.org/10.1016/j.geomorph.2009.11.023, 2010.

Mayer, T., Eppes, M., and Draebing, D.: Influences driving and limiting the efficacy of ice segregation in alpine rocks, Geophys. Res. Lett., 50, e2023GL102951, https://doi.org/10.1029/2023GL102951, 2023.

McAllister, D., Warke, P., and McCabe, S.: Stone temperature and moisture variability under temperate environmental conditions: Implications for sandstone weathering, Geomorphology, 280, 137–152, https://doi.org/10.1016/j.geomorph.2016.12.016, 2017.

McCormick, E. L., Dralle, D. N., Hahm, W. J., Tune, A. K., Schmidt, L. M., Chadwick, K. D., and Rempe, D. M.: Widespread woody plant use of water stored in bedrock, Nature, 597, 225–229, https://doi.org/10.1038/s41586-021-03761-3, 2021.

Mitchell, A. and Sass, O.: Rock weathering: The effects of varying rock moisture on controlled weathering cycles in low porosity limestone, Geomorphology, 457, 109149, https://doi.org/10.1016/j.geomorph.2024.109149, 2024.

Murray, J.: Anatomical features in the roots of the genus Primula, in: Transactions of the Botanical Society of Edinburgh, 31, 323–326, https://doi.org/10.1080/13594863409441354, 1934.

Murton, J. B., Peterson, R., and Ozouf, J. C.: Bedrock fracture by ice segregation in cold regions, Science, 314, 1127–1129, https://doi.org/10.1126/science.1132127, 2006.

Ni, J., Cheng, Y., Wang, Q., Ng, C. W. W., and Garg, A.: Effects of vegetation on soil temperature and water content: Field monitoring and numerical modelling, J. Hydrol., 571, 494–502, https://doi.org/10.1016/j.jhydrol.2019.02.015, 2019.

Nie, Y. P., Chen, H. S., Ding, Y. L., Zou, Q. Y., Ma, X. Y., and Wang, K. L.: Qualitative identification of hydrologically different water sources used by plants in rock-dominated environments, J. Hydrol., 573, 386–394, https://doi.org/10.1016/j.jhydrol.2019.03.004, 2019.

Orr, S. A., Fusade, L., Young, M., Stelfox, D., Leslie, A., Curran, J., and Viles, H.: Moisture monitoring of stone masonry: a comparison of microwave and radar on a granite wall and a sandstone tower, J. Cult. Herit., 41, 61–73, https://doi.org/10.1016/j.culher.2019.07.008, 2020.

Pawlik, Ł., Phillips, J. D., and Šamonil, P.: Roots, rock, and regolith: Biomechanical and biochemical weathering by trees and its impact on hillslopes–A critical literature review, Earth-Sci. Rev., 159, 142–159, https://doi.org/10.1016/j.earscirev.2016.06.002, 2016.

Phillips, J. D.: Biogeomorphology and contingent ecosystem engineering in karst landscapes, Prog. Phys. Geogr., 40, 503–526, https://doi.org/10.1177/0309133315624641, 2016.

Piuzzi, E., Pittella, E., Pisa, S., Cataldo, A., De Benedetto, E., and Cannazza, G.: An improved noninvasive resonance method for water content characterization of Cultural Heritage stone materials, Measurement, 125, 257–261, https://doi.org/10.1016/j.measurement.2018.04.013, 2018.

Poot, P., Hopper, S. D., and van Diggelen, J. M.: Exploring rock fissures: does a specialized root morphology explain endemism on granite outcrops?, Ann. Bot., 110, 291–300, https://doi.org/10.1093/aob/mcs097, 2012.

Porder, S.: How plants enhance weathering and how weathering is important to plants, Elements, 15, 241–246, https://doi.org/10.2138/gselements.15.4.241, 2019.

Raevel, V., Munoz, F., Pons, V., Renaux, A., Martin, A., and Thompson, J. D.: Changing assembly processes during a primary succession of plant communities on Mediterranean roadcuts, J. Plant Ecol., 6, 19–28, https://doi.org/10.1093/jpe/rts017, 2013.

Raunkiaer, C.: The life forms of plants and statistical plant geography; being the collected papers of C. Raunkiaer, Copenhagen, https://archive.org/details/in.ernet.dli.2015.271790 (last access: 12 May 2026), 1934.

Ravaji, B., Alí-Lagoa, V., Delbo, M., and Wilkerson, J. W.: Unraveling the mechanics of thermal stress weathering: Rate-effects, size-effects, and scaling laws, J. Geophys. Res.-Planet, 124, 3304–3328, https://doi.org/10.1029/2019JE006082, 2019.

Rempe, D. M. and Dietrich, W. E.: Direct observations of rock moisture, a hidden component of the hydrologic cycle, P. Natl. Acad. Sci. USA, 115, 2664–2669, https://doi.org/10.1073/pnas.1800141115, 2018.

Sass, O.: Rock moisture fluctuations during freeze-thaw cycles – preliminary results derived from electrical resistivity measurements, Polar Geogr., 28, 13–31, https://doi.org/10.1080/789610205, 2004.

Sass, O.: Rock moisture measurements: techniques, results, and implications for weathering, Earth Surf. Proc. Land.: The Journal of the British Geomorphological Research Group, 30, 359–374, https://doi.org/10.1002/esp.1190, 2005.

Sass, O.: Investigating rock moisture at a sandstone massif in the Saxonian Switzerland climbing area, J. Geomorphol., https://doi.org/10.1127/jgeomorphology/2022/0711, 2022.

Sass, O. and Heil, S.: The role of moisture and salt distribution in the weathering of the medieval cave town of Uplistsikhe, Georgia, Heritage Sci., 12, 2024, https://doi.org/10.1186/s40494-024-01310-5, 2024.

Sass, O. and Kloss, S.: Distribution of macro charcoal from forest fires in shallow soils of the Northern Alps, J. Soils Sediment., 15, 748–758, https://doi.org/10.1007/s11368-014-0954-9, 2015.

Sass, O. and Sarcletti, S.: Patterns of long-term regeneration of forest fire slopes in the Northern European Alps – a logistic regression approach, Geogr. Ann. A, 99, 56–71, https://doi.org/10.1111/geoa.12136, 2017.

Sass, O. and Viles, H.: Heritage hydrology: a conceptual framework for understanding water fluxes and storage in built and rock-hewn heritage, Heritage Sci., 10, 66, https://doi.org/10.1186/s40494-022-00693-7, 2022.

Sass, O. and Viles, H. A.: Wetting and drying of masonry walls: 2D-resistivity monitoring of driving rain experiments on historic stonework in Oxford, UK, J. Appl. Geophys., 70, 72–83, https://doi.org/10.1016/j.jappgeo.2009.11.004, 2010.

Sass, O., Heel, M., Hoinkis, R., and Wetzel, K. F.: A six-year record of debris transport by avalanches on a wildfire slope (Arnspitze, Tyrol), Z. Geomorphol., 54, 181–193, https://doi.org/10.1127/0372-8854/2010/0054-0009, 2010.

Sass, O., Stöger, F., Weber, F., Juraschek, R., and Sarcletti, S.: Die Regeneration der Waldbrandhänge des Karwendelgebirges–Bestandsaufnahme und Ermittlung der Steuerfaktoren, Innsbrucker Geogr. Stud., 41, 129–177, ISBN 978-3-901182-44-0, 2019.

Sass, O., Bauer, U., Deola, T., and Jentsch, A.: How does biotic weathering work? Influence of alpine plants on rock temperature and rock moisture – dataset (0.0.0), Zenodo [data set], https://doi.org/10.5281/zenodo.17768495, 2025.

Schrott, L. and Sass, O.: Application of field geophysics in geomorphology: advances and limitations exemplified by case studies, Geomorphology, 93, 55–73, https://doi.org/10.1016/j.geomorph.2006.12.024, 2008.

Starke, J., Ehlers, T. A., and Schaller, M.: Latitudinal effect of vegetation on erosion rates identified along western South America, Science, 367, 1358–1361, https://doi.org/10.1126/science.aaz0840, 2020.

Suryanto, B., Saraireh, D., Kim, J., McCarter, W. J., Starrs, G., and Taha, H. M.: Imaging water ingress into concrete using electrical resistance tomography, Int. J. Adv. Eng. Sci. Appl. Math., 9, 109–118, https://doi.org/10.1007/s12572-017-0190-9, 2017.

Vacik, H., Arndt, N., Arpaci, A., Koch, V., Mueller, M., and Gossow, H.: Characterisation of forest fires in Austria, Aust. J. For. Sci., 128, 1–31, https://www.researchgate.net/publication/233427633_Characterisation_of_forest_fires_in_Austria (last access: 12 May 2026), 2011.

Viles, H. A., Naylor, L. A., Carter, N. E. A., and Chaput, D.: Biogeomorphological disturbance regimes: progress in linking ecological and geomorphological systems, Earth Surf. Proc. Land., 33, 1419–1435, https://doi.org/10.1002/esp.1717, 2008.

Weast, R. C., Astle, M. J., and Beyer, W. H.: Handbook of Chemistry and Physics, Library of Congress, 69. Ed., CRC Press, Boca Raton, Florida, ISBN 0849304695, 1989.

Weiss, T. and Sass, O.: The challenge of measuring rock moisture – a laboratory experiment using eight types of sensors, Geomorphology, 416, 108430, https://doi.org/10.1016/j.geomorph.2022.108430, 2022.

Witty, J. H., Graham, R. C., Hubbert, K. R., Doolittle, J. A., and Wald, J. A.: Contributions of water supply from the weathered bedrock zone to forest soil quality, Geoderma, 114, 389–400, https://doi.org/10.1016/S0016-7061(03)00051-X, 2003.

Yang, X., Wang, J., Hou, D., Zhu, C., and He, M.: Effect of dry-wet cycling on the mechanical properties of rocks: a laboratory-scale experimental study, Processes, 6, 199, https://doi.org/10.3390/pr6100199, 2018.

Zwieniecki, M. A. and Newton, M.: Roots growing in rock fissures: their morphological adaptation, Plant Soil, 172, 181–187, https://doi.org/10.1007/BF00011328, 1995.